Geotechnical Testing Journal, Vol. 26, No. 2
Paper ID GTJ9916_262
Available online at: www.astm.org

Fangsheng Shuai,[1] *D. G. Fredlund,*[2] *and L. Samarasekera*[3]

Numerical Simulation of Water Movement in the Suction Equalization of a Thermal Conductivity Sensor

ABSTRACT: Laboratory and field measurements of soil suction using a thermal conductivity soil suction sensor involves installing the sensors into a soil mass. The sensors may be installed either in an initially wet or an initially dry state. In order to ensure a reliable suction measurement, it is important that the sensor reach suction equalization with the surrounding soil. The results of a numerical study have shown that, in most cases, the equalization time required for an initially dry sensor is less than the equalization time for an initially wet sensor. This difference is mainly due to the unsaturated zone that develops on the boundary of the initially wet sensor at the beginning of the drying process. The results of the numerical simulation have been substantiated by laboratory suction measurements.

KEYWORDS: soil suction, soil suction measurement, equalization time, thermal conductivity soil suction sensor, numerical modeling

The thermal conductivity soil suction sensor appears to hold significant promise for the routine in situ measurement of soil suction. The sensors provide an indirect measurement of soil suction, the state variable required to understand and describe the mechanical behavior of unsaturated soils.

A thermal conductivity soil suction sensor consists of a temperature- sensing element and a miniature heater embedded in a standard porous ceramic block. A schematic diagram of a thermal conductivity soil suction sensor is shown in Fig. 1. During operation, the heating element in the sensor is subjected to a standard heat pulse, and the temperature rise in the sensor with time is measured. Since the thermal conductivity of water is approximately 20 times higher than that of air, the temperature increase in the sensor due to the heat pulse is related to the water content of the standard ceramic. The water content of the ceramic is, in turn, closely related to the suction of the ceramic, which is assumed to be equal to the soil suction in the surrounding soil after equilibrium has been established. Therefore the temperature change inside the sensor subsequent to the heat pulse can be used as a measure of the soil suction in the surrounding soil.

Thermal conductivity sensors have been used for several decades for the measurement of soil suction and have shown consistent, reproducible, and stable output reading with time (Fredlund and Wong 1989). However, the performance of thermal conductivity soil suction sensors in terms of their strength and durability in the field has been disappointing (Fredlund et al. 1994). The range over which suction could be made has also been limited (Fredlund et al. 1994). A recent research program at the University of Saskatchewan, Saskatoon, has resulted in the development of a new prototype thermal conductivity soil sensor (Fredlund et al. 1998) that overcomes many of the limitations and difficulties previously encountered with commercially available thermal conductivity sensors.

The measurements obtained for soil suction, when using the thermal conductivity sensor, are meaningful only if the soil and the sensor have reached a state of equilibrium (or equalization). Under these conditions the suction measured by the sensor is the same as the suction in the soil. Previous numerical modeling studies on the thermal conductivity sensors have examined the heat flow mechanism involved when making the thermal conductivity measurements (Xing and Fredlund 1994).

This study focuses on the hydraulic conductivity dependency of the sensor as it goes toward equilibrium with respect to the soil suction in the surrounding soil. A finite element seepage model was used to predict the movement of water between the soil and the sensor as a part of the equalization process. The study provides information on the behavior of the thermal conductivity soil suction sensor when it is either drier than or wetter than the surrounding soil. Numerical simulations do not replace the need for field or laboratory studies but provide the engineer with valuable information for the design and interpretation of laboratory or field studies. These predictive techniques also provide a useful tool in the design of the thermal conductivity sensor.

Suction Equalization between the Sensor and the Soil

The process by which the sensor comes into equilibrium with the suction in the surrounding soil, within an acceptable tolerance, is termed suction equalization. The time required for the sensor to come to equilibrium with surrounding soil is mainly dependent on the coefficient of permeability and the soil-water characteristic of the ceramic and the soil. The flows of water within and around a sensor are governed by the principles of seepage through an

Received August 24, 2002; accepted for publication May 3, 2002; published May 14, 2003.

[1] Research engineer, Department of Civil Engineering, University of Saskatchewan, Saskatoon, SK, Canada, S7N 5A9.
[2] Professor Emeritus of civil engineering, Department of Civil Engineering, University of Saskatchewan, Saskatoon, SK, Canada, S7N 5A9.
[3] Research officer, Department of Civil Engineering, University of Saskatchewan, Saskatoon, SK, Canada, S7N 5A9.

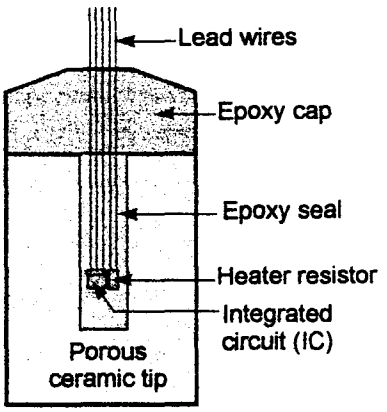

FIG. 1—*A schematic diagram of a thermal conductivity soil suction sensor.*

unsaturated medium. For an isotropic material, the governing equation of transient seepage can be written as follows.

$$k(\psi)\nabla^2 h = \frac{\partial \theta_w(\psi)}{\partial t} \tag{1}$$

where

ψ = soil suction,

h = total head, (i.e., $\frac{u_w}{\rho_w g} + Y$ where u_w = pore-water pressure, ρ_w = density of water, g = gravitational acceleration, and Y = elevation head).

$k(\psi)$ = coefficient of permeability of the isotropic material as a function of suction,

$\theta_w(\psi)$ = volumetric water content, and

t = elapsed time.

For unsaturated materials (i.e., sensor as well as the soil), the coefficient of permeability is not a constant but is a function of soil suction. Soil suction is, in turn, a function of the water content of the material. Fredlund et al. (1994) proposed the use of a permeability function generated through the integration from saturated soil conditions (i.e., saturated coefficient of permeability and saturated volumetric water content) along the soil-water characteristic curve. Fredlund and Xing (1994) suggested the following mathematical equation to describe the relationship between soil suction and volumetric water content:

$$\theta(\psi) = C(\psi)\frac{\theta_s}{[\ln\{e + (\psi/a)^n\}]^m} \tag{2}$$

where:

θ_s = saturated volumetric water content,

e = base of natural log, 2.718.....,

a = soil parameter related to the air entry value of the soil, and

n = soil parameter related to the slope of the soil-water characteristic.

ve at the inflection point,

m = soil parameter related to the residual water content, and

$C(\psi)$ = correction factor to ensure that the soil-water characteristic curve passes through 1 000 000 kPa at zero water content.

The governing equation for seepage, along with appropriate boundary condition and initial conditions, can be solved numerically using the finite element method. The equations for the soil-water characteristic curve and the permeability function are substituted into the governing equation of flow (i.e., Eq 1).

Numerical Modeling of Suction Equalization

The time required for the sensor to reach equalization is dependent on the coefficient of permeability and the water storage capacity of the ceramic and the surrounding soil. A numerical analysis of water flow between the ceramic tip and the surrounding soil was conducted. The influence of the water coefficient of permeability and the soil-water characteristic curve of the ceramic tip and the soil on the response time of the sensor was studied. The numerical simulation studies can be divided into the following parts. First, the sensor calibration process was simulated in order to investigate the influence of the hydraulic properties of the ceramic tip on the equilibrium time. Then, the simulation results obtained during the above study were used in the simulation of various hydraulic properties of the surrounding soil. Finally, the results from both of the above simulations were used in an additional simulation related to the drying or wetting processes. The results showed why there was a difference in the equilibrium time during the drying and the wetting processes.

Simulation of the Calibration Process

The thermal conductivity soil suction sensor must be calibrated before being used to measure soil suction. The calibration can be performed by applying a range of suction values to sensors installed in a modified pressure plate apparatus. The calibration procedure is illustrated in Fig. 2. The sensor is set on a thin layer of contact material placed on the high air entry plate (Fig. 3). The contact material on the high air entry plate provides continuity between the water in the porous ceramic tip and water in the high air entry plate. As a result, continuous hydraulic flow between the ceramic of sensor and the water chamber below the high air entry plate can be maintained. The suction is applied by increasing the air pressure in the pressure plate apparatus while maintaining the water pressure below the high air entry plate at atmosphere pressure. The suction measured when using the sensor can be monitored periodically until suction equilibrium is achieved. The final reading of soil suction, after equalization has been attained, is taken as the calibration value. The above procedure was repeated for various applied suctions ranging from 0 to 400 kPa in order to obtain a complete calibration curve. Typical time response curves of a thermal conductivity soil suction sensor for changes in applied suction, during the calibration process, are shown in Fig. 4.

The time required for sensors to reach equalization during the calibration process depends mainly on factors such as the permeability function and the soil-water characteristic curve for the ceramic tip. The coefficient of permeability of the high air entry ceramic plate and the properties of the contact material may also have some influence on the results.

Finite Element Discretization, Initial and Boundary Conditions—The water flow and suction change during sensor calibration was simulated using Seep/W software. Seep/W is a

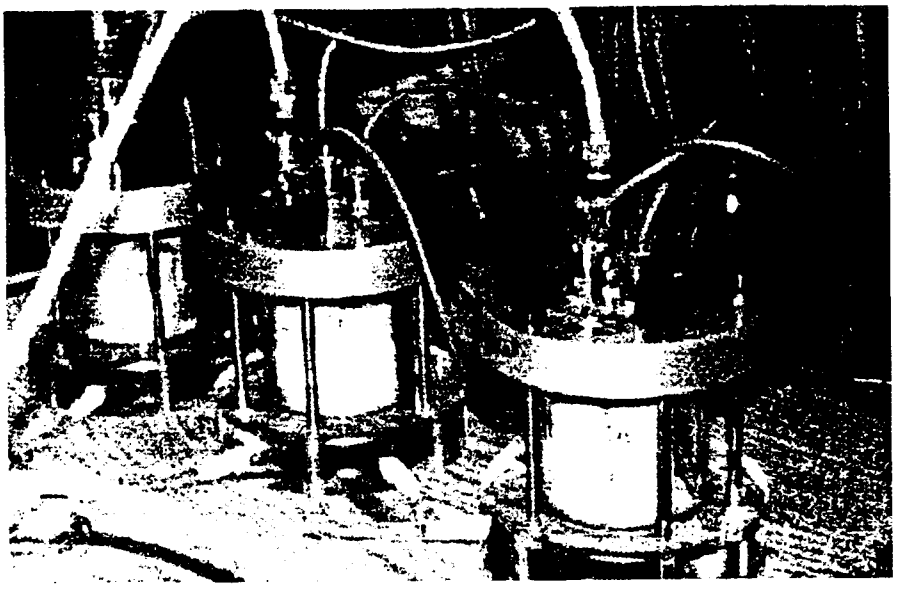

FIG. 2—*Pressure plate calibration setup with three sensors per cell.*

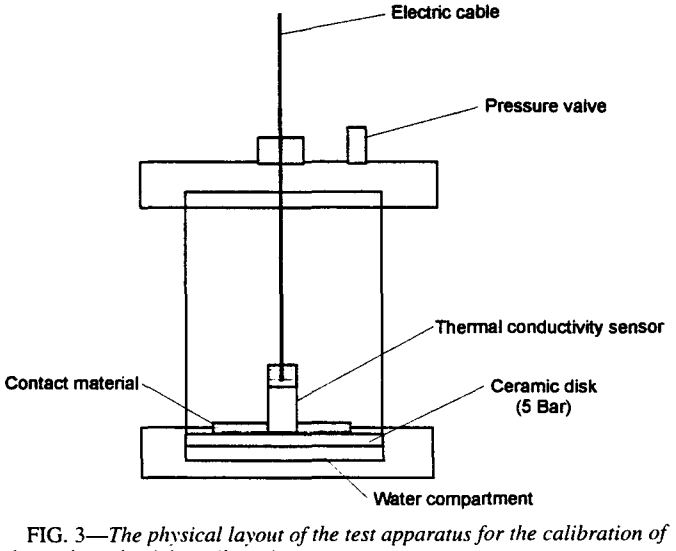

FIG. 3—*The physical layout of the test apparatus for the calibration of thermal conductivity soil suction sensors.*

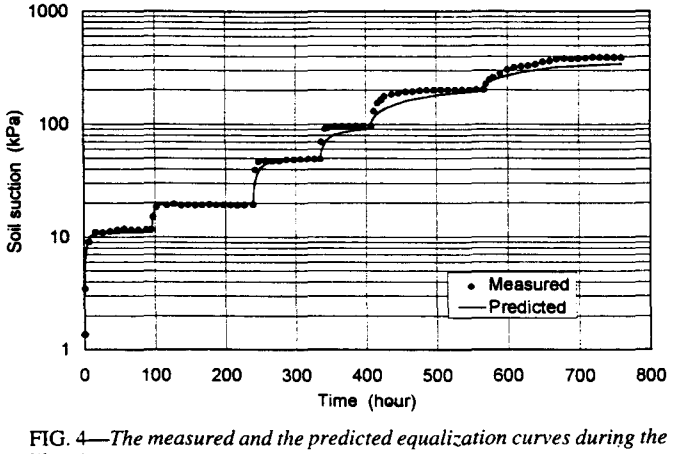

FIG. 4—*The measured and the predicted equalization curves during the calibration process.*

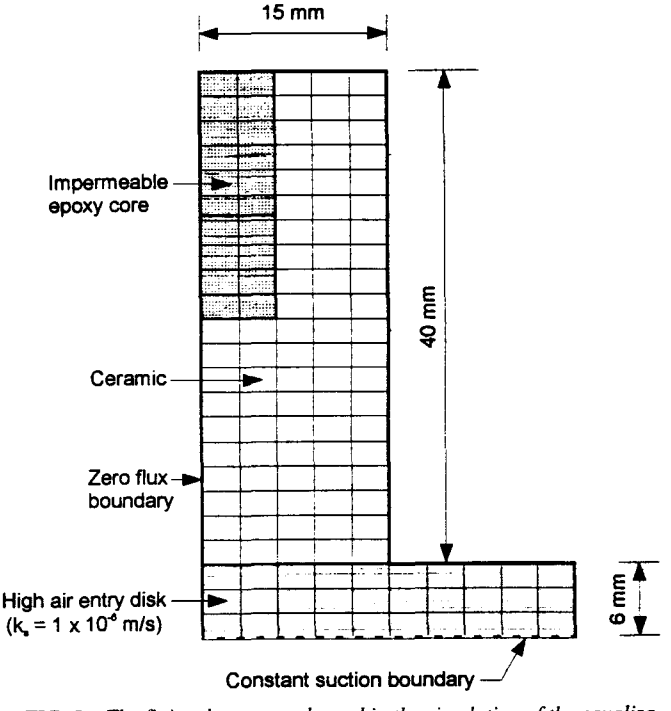

FIG. 5—*The finite element mesh used in the simulation of the equalization process during calibration.*

two-dimensional finite element software that can simulate saturated and unsaturated flow and also accommodate transient and steady state flow.

A two-dimensional, axi-symmetric transient model was used for transient and steady state simulations. The finite element mesh is shown in Fig. 5. The ceramic material, the epoxy core, and the high air entry disk are discretized using four-noded axi-symmetric elements as separate materials. The contact material was not taken into consideration during modeling since the thickness of the contact material was small (i.e., about 1 mm) in comparison to the thickness of the high air entry plate (i.e., 6 mm).

All boundaries, except the bottom boundary of the high air entry ceramic plate, were specified as zero-flux boundaries. A suction equal to the applied suction during calibration was maintained at the bottom boundary. For the first simulation, the sensor was assumed be saturated, and hence the suction throughout the sensor was set to zero. For subsequent simulations, the suction in the sensor was considered to be equal to the equalized value of suction from the previous analysis step. The average of suctions from each node of the sensor was assumed to be the suction value of the sensor.

Material Characterization—The soil-water characteristic curve and the permeability function used for the ceramic material are shown in Figs. 6*a* and 6*b*, respectively. The soil-water characteristic curve was measured in the soil laboratory at the University of Saskatchewan, Saskatoon, Saskatchewan. The permeability function was computed indirectly from the measured soil-water characteristic curve and the saturated coefficient of permeability of the ceramic (Fredlund et al. 1994). The saturated coefficient of permeability was measured using the falling head permeability test in the soil laboratory of the University of Saskatchewan.

The water content versus soil suction curves (i.e., the soil-water characteristic curves) for the ceramic tip shown in Fig. 6 is not the same during wetting and drying. The hysteresis in the soil-water characteristics of the ceramic tip may cause hysteresis in the sensor response upon wetting and drying. The entire calibration process is a drying process, and only the drying portion of the soil-water characteristic curve and the permeability function was used in the modeling.

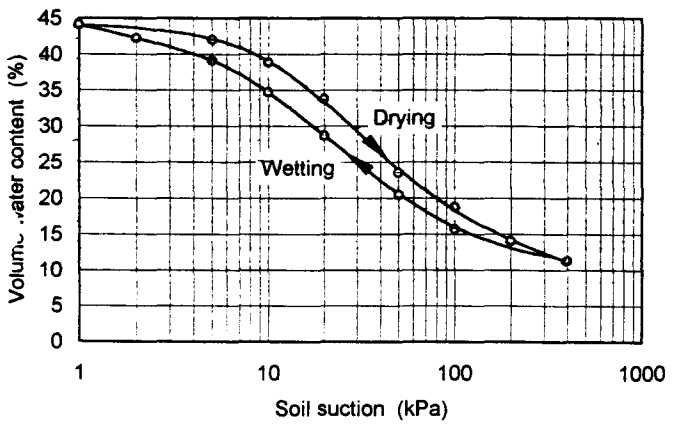

(a) The soil-water characteristic curve

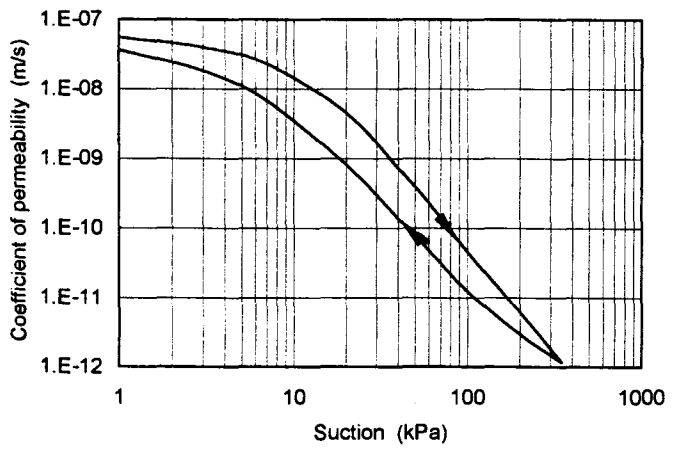

(b) The permeability function

FIG. 6—*Hydraulic properties of the ceramic used for the soil suction sensor (obtained from the soil-water characteristic curve).*

The air entry value of the high air entry disk is higher than 500 kPa, which is much higher than the maximum applied suction (i.e., 400 kPa) during calibration, and therefore a saturated coefficient of permeability of 1.21×10^{-9} m/s was applicable throughout the calibration study. The saturated coefficient of permeability of the high air entry disk was obtained from values published by Soilmoisture Equipment Corp., Santa Barbara, CA. The epoxy core was considered to be essentially impermeable (i.e., $k = 1.0 \times 10^{-18}$ m/s).

Presentation of Results on Laboratory Calibration Simulations—Computed equilibrium curves are presented in Fig. 4 along with the measured equilibrium curves during calibration. The consistency between the measured and computed equilibrium curves was good when the applied suctions were lower than 100 kPa. A discrepancy was observed when the applied suctions were higher than 100 kPa. The predicted equalization times were longer than the measured equilibrium time. The discrepancy may partly be due to flow taking place along the surface of the sensor ceramic during the test. For the modeling of the sensor, all drainage from the sensor was assumed to take place at the bottom of the ceramic plate, and this may not be what happens during the laboratory calibration. The side drainage would reduce the time required for equalization. The influence of the contact material was not taken into consideration during the modeling simulation but may also attribute to the discrepancy.

Both measured and predicted equalization times under different applied suctions are listed in Table 1. The results show that the higher the applied suction, the longer the equalization time. Consequently, the time required for the sensor to reach equilibrium increases with increasing applied suctions. This phenomenon becomes more accentuated in the higher suction range. When the applied suctions are lower than 100 kPa, the time required for sensors to reach equalization is less than 48 h, while the equalization time increases to more than 100 h when the applied suctions increase to 200 and 400 kPa. The increase in the equalization time with an increase in applied suction is mainly due to the decrease in the coefficient of permeability of the ceramic with increasing suction.

Simulation of the Equalization Process during Suction Measurement

When a sensor is installed into the soil, the equalization time will not only be affected by the hydraulic properties of the ceramic tip but also by the hydraulic properties of the surrounding soil. The

TABLE 1—*The equalization time required under different applied suctions.*

Suction Change	Equalization Time, h	
	Measured	Predicted
0 to 11 kPa	29	40
11 to 20 kPa	44	44
20 to 50 kPa	45	50
50 to 100 kPa	46	65
100 to 200 kPa	82	140
200 to 400 kPa	153	220

effect of the surrounding soil on the equalization time was studied using a finite element simulation. The hydraulic properties of the ceramic tip used for the calibration process were the same as those used in the above computer simulations.

Finite Element Discretization and Boundary Conditions—The finite element model used for the analysis is shown in Fig. 7. A two-dimensional axi-symmetric transient model was used. A zero flux boundary was applied along the centerline of the sensor. The remaining boundaries were considered to be infinite and modeled using infinite elements. The finite element mesh consists of four-node rectangular or three-node triangular elements.

Material Characterization—Three types of soil, namely, sand, silt, and Regina clay, were used for the modeling simulation. The soil-water characteristic curves for the three soils along with the measured soil-water characteristic curve for the ceramic tip are shown in Fig. 8*a*. The soil-water characteristic curves for the sand and Regina clay were obtained from SoilVision's knowledge-based system (Fredlund 1999).

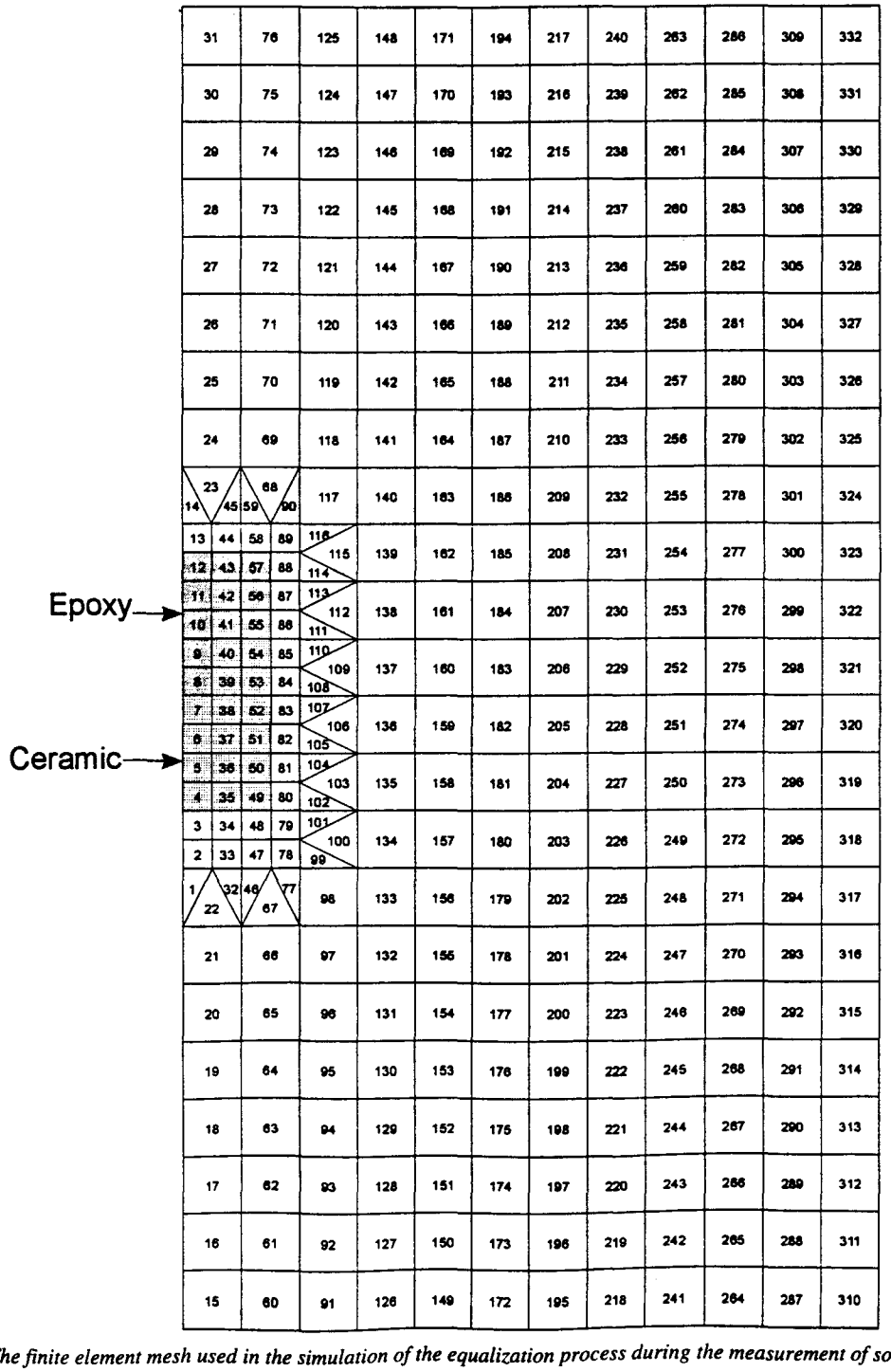

FIG. 7—*The finite element mesh used in the simulation of the equalization process during the measurement of soil suction.*

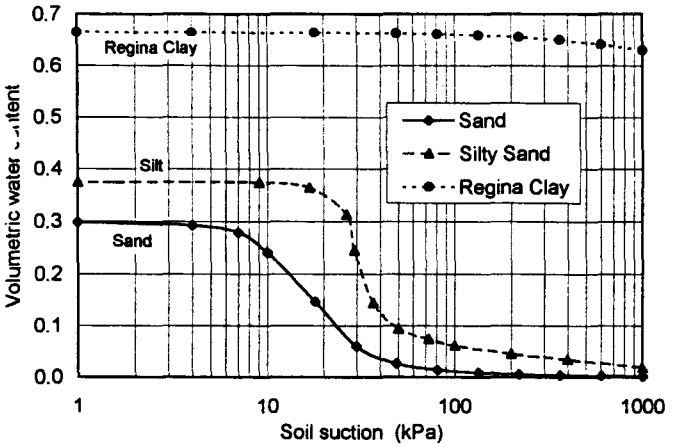

(a) The soil-water characteristic curve.

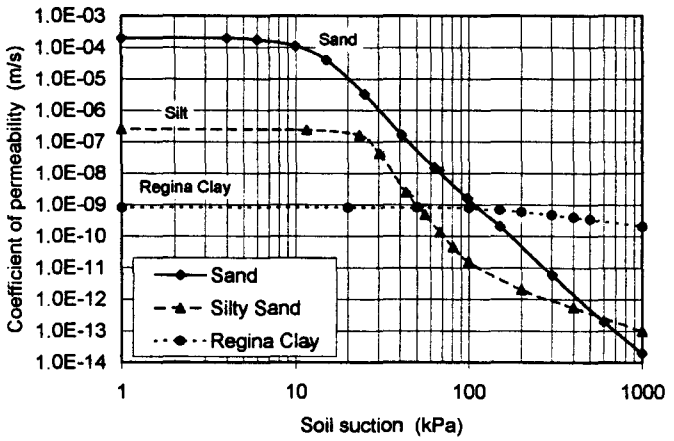

(b) The permeability function

FIG. 8—*The hydraulic properties of three soils used in the modeling study.*

The permeability functions for the three soils are shown in Fig. 8*b*, along with the permeability function for the ceramic tip. The permeability functions for the soils were determined from soil-water characteristic curves using the Green and Corey (1971) procedure for converting the soil-water characteristic curve and the saturated coefficient of permeability into a permeability function. Material characterization of the sensor is the same as that used for the simulation of the calibration process. However, the wetting portion of the soil-water characteristic curve and permeability function of the ceramic was also used to model the wetting process (i.e., the process in which an initially dry sensor equalizes with the surrounding soil).

Analysis and Results—The transient water flow and suction change process during suction equalization was numerically simulated using the Seep/W finite element program. Two hydraulic processes were simulated for each of the three soils. One is the wetting process and the other is the drying process. In the wetting process, a saturated sensor was installed into the soil to simulate the equilibrium process with the surrounding soil. The initial suction in the saturated ceramic tip was assumed to be 0 kPa. In the drying process, a dry sensor was inserted into the soil to simulate the equalization process with the soil. The initial suction for the dry sensor was assumed to be 400 kPa. For each process, three different initial soil suction values (i.e., 100, 200, and 300 kPa) were assumed for the surrounding soil, respectively, to investigate the influence of the initial suction conditions on the response time of the sensors.

The suction equalization curves for the sand are shown in Fig. 9*a*. The results indicate that at high suctions (e.g., greater than 100 kPa) the equalization time required for the initially dry sensor is less than the equalization time required for a saturated sensor.

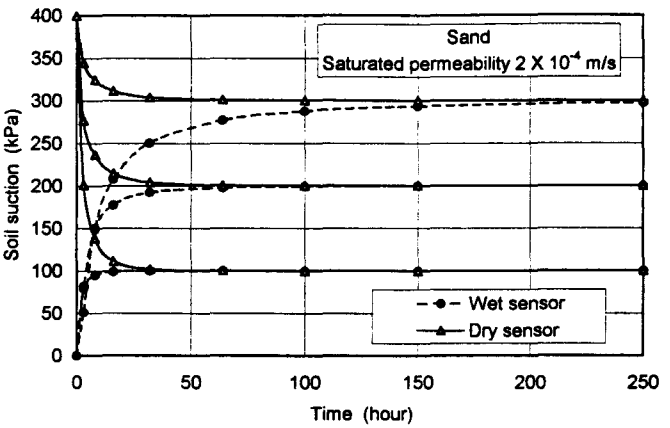

(a) Computed soil suction equalization for a sand.

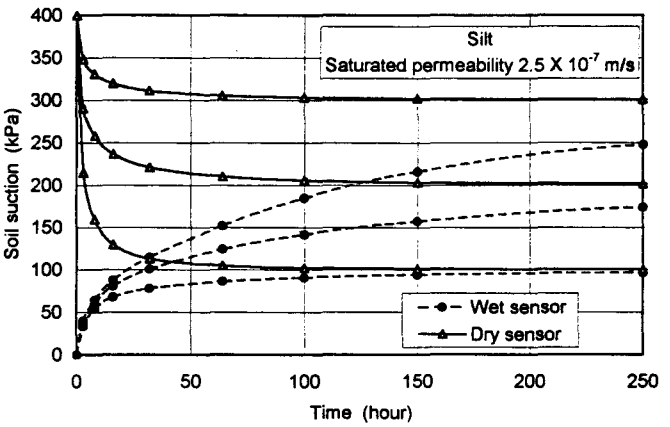

(b) Computed soil suction equalization for a silty sand.

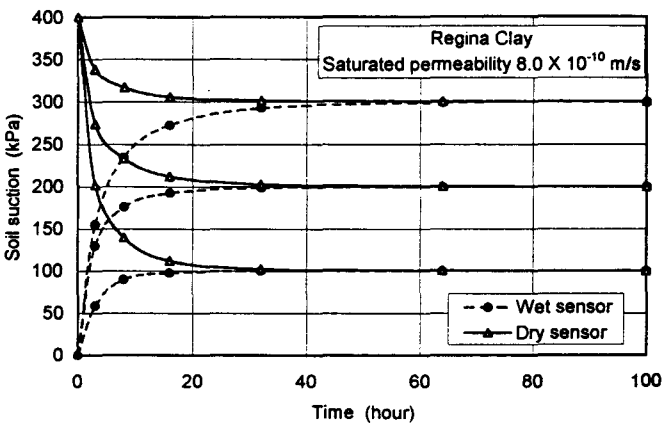

(c) Computed soil suction equalization for Regina clay.

FIG. 9—*The predicted suction equalization curves for three soils.*

When the initial suction of the soil is 200 kPa, the initially dry sensor required 50 h to equalize, whereas the initially wet sensor required about 100 h. The time difference between wet and dry sensor simulations becomes more accentuated when the suction in the surrounding soil is higher than 300 kPa. Similar observations were made during several laboratory tests when using the AGWA-II thermal conductivity sensors (Sattler and Fredlund 1989). The test results on the Regina clay are shown in Fig. 10. The equalization times for the initially dry sensor were about 50 h, whereas the time for the initially wet sensor was more than 200 h.

The predicted suction equalization curves for the silt are shown in Fig. 9*b*. The equalization times required for sensors to reach equilibrium in the silt were much longer than the times required for the sand under the similar condition. The longer equalization times are attributable to the lower coefficient of permeability and higher water storage change related to a change of suction. Similar observations were made during laboratory suction measurement (Sattler and Fredlund 1989), and results are shown in Fig. 11. In addition, a considerably longer equalization time was required for the sensor to equilibrate when the soil suction in the silt was high. The equilibrium time for a initially wet sensor to reach equalization was more than 500 h for the silt when the soil suction was about 300 kPa. Under this condition, an initially dry sensor will significantly reduce the time required for equalization. The equalization time for a dry sensor is less than 100 h.

The observation that the equalization time required for the initially dry sensor was less than the equalization time for an initially wet sensor at high suction was also noted for Regina clay as shown in Fig. 10, but the effect was less significant than that for the silt.

Comparison between Laboratory Test Results and Computer Simulations—The difference in the equalization time required for an initially dry sensor versus an initially wet sensor has also been observed during other laboratory suction measurements when using thermal conductivity soil suction sensors (Sattler and Fredlund 1989; Fredlund and Shuai 1999). The measured equalization curves from one test are shown in Fig. 12. The measurements were conducted using two sensors inserted into a soil specimen. The soil specimen was a compacted Indian Head till with an initial water content of 16%. One sensor was initially wet, while the another was initially air dry. The sensors were inserted into predrilled holes in either end of the specimen. The soil specimen with the installed sensors was then wrapped with aluminum foil and sealed using masking tape to minimize moisture loss. The responses from both sensors were monitored immediately and at various elapsed times after installation until equilibrium was attained.

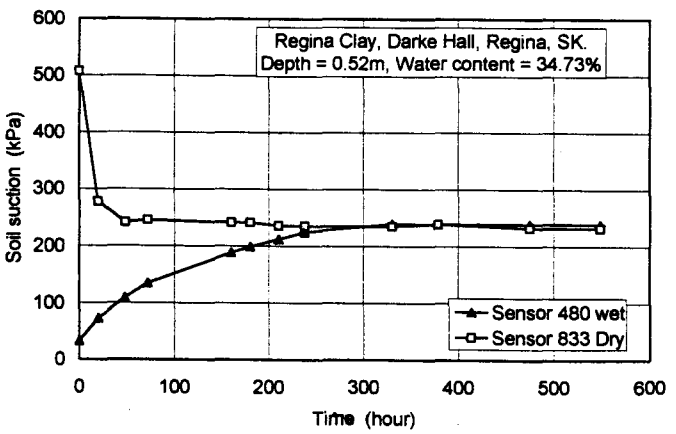

FIG. 10—*Experimental suction equalization for Regina clay (from Sattler and Fredlund, 1989).*

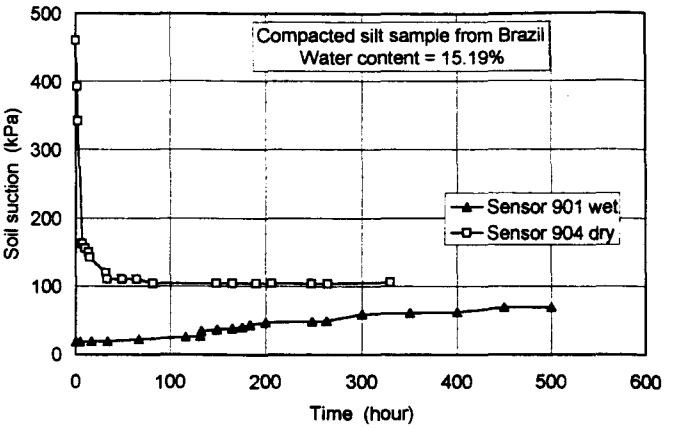

FIG. 11—*Experimental soil suction equalization for a compacted silt from Brazil (from Sattler and Fredlund, 1989).*

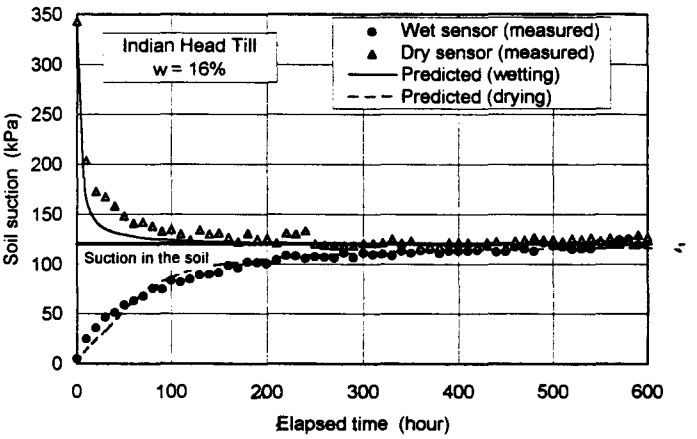

FIG. 12—*The measured and the predicted suction equalization curves for Indian Head till.*

The finite element numerical model was used to simulate the equilibrium process. The soil-water characteristic curves and permeability functions for Indian Head till used in the modelling are shown in Figs. 13*a* and 13*b*. Soil-water characteristic curves were obtained from the SoilVision database developed by M. Fredlund (Fredlund 1999). The permeability function was determined by using the Fredlund-Xing equation (1994) by converting the soil-water characteristic curve, along with the saturated coefficient of permeability, into a permeability function. The saturated coefficient of permeability was assumed based on measured saturated coefficients of permeability for the Indian head till (Wong 1985). The measured saturated coefficient of permeability was 9.6×10^{-11} m/s under a backpressure of 200 kPa. Since no backpressure was applied during the laboratory test, the saturated coefficient of permeability of the specimen should be lower than that measured due to entrapped air bubbles. A saturated coefficient of permeability of 1.0×10^{-11} was assumed for the Indian Head till simulations.

A comparison between the predicted and measured equalization curves is presented in Fig. 12. Reasonably good agreement can be observed between the predicted and measured equalization curves. Both results indicated that the initially wet sensor has

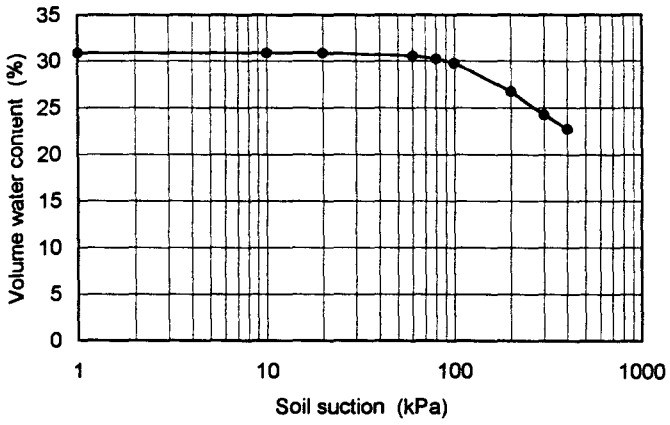

(a) The soil-water characteristic curve

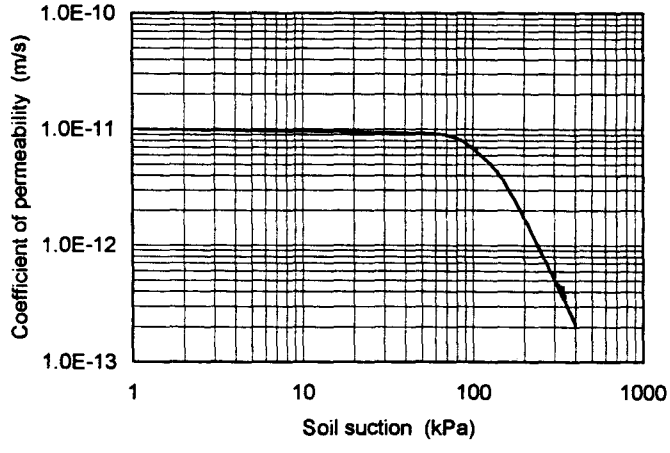

(b) The permeability function

FIG. 13—*The hydraulic properties of Indian Head till used in the modeling study (obtained from the soil-water characteristic curve).*

longer equalization times (i.e., maximum 400 h) than the initially dry sensor (i.e., 200 h). Some departures were noted during the first stage of the equalization process between the predicted equalization curves and the measured equalization curves. However, considering that the properties of the soil specimen used in the modeling were assumed rather than measured, the departures were as anticipated.

Discussion of the Equalization Process Results

The measured and the predicted equalization process indicated that a dry sensor is more likely to reach suction equalization faster than a initially wet sensor. In order to identify the reason behind this phenomenon, additional modeling of the equalization process, associated with the drying or wetting process of a thermal conductivity sensor, was undertaken.

The two-dimensional axi-symmetric transient model shown in Fig. 14 was used for this simulation. In order to simplify the problem, a pre-determined suction (i.e., 200 kPa for drying and 0 kPa for wetting) was directly applied to the bottom of an initially dry or wet sensor during modeling. Other boundaries were specified as zero flux boundary. The permeability functions and soil-water characteristic curves were the same as those used in the previous modeling of the ceramic.

The suction equalizations with time predicted for both wet and dry sensors are shown in Fig. 15. The rate of suction change in the dry sensor is more rapid and comes to suction equalization faster than the wet sensor even though the suction changes during the equalization process are the same for both sensors (i.e., from 0 to 200 kPa for the wet sensor and 200 to 0 kPa for the dry sensor). The results show that an unsaturated zone developed at the boundary of the initially wet sensor at the beginning of the drying process (Fig. 16*a*). The low permeability in the unsaturated zone prevents water inside the wet sensor from flowing out, resulting in a longer equalization time. On the other hand, no such unsaturated zone develops during the wetting process for the initially dry sensor (Fig. 16*b*). As

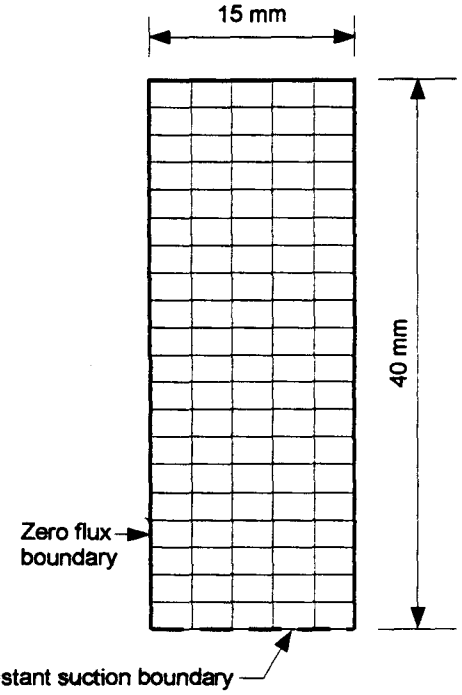

FIG. 14—*The finite element mesh and the assumed boundary conditions used in the modeling study.*

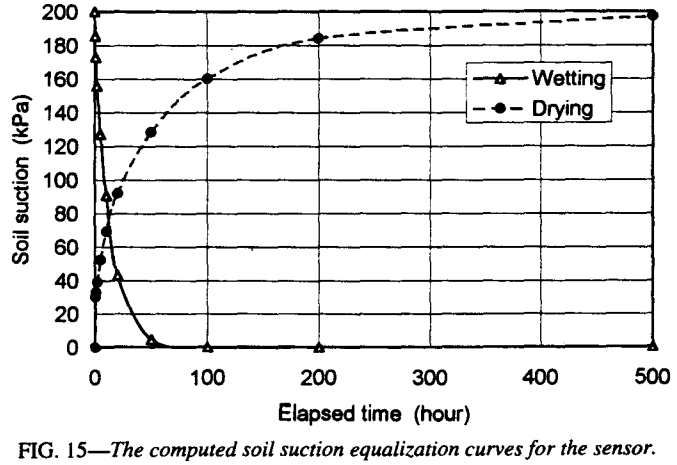

FIG. 15—*The computed soil suction equalization curves for the sensor.*

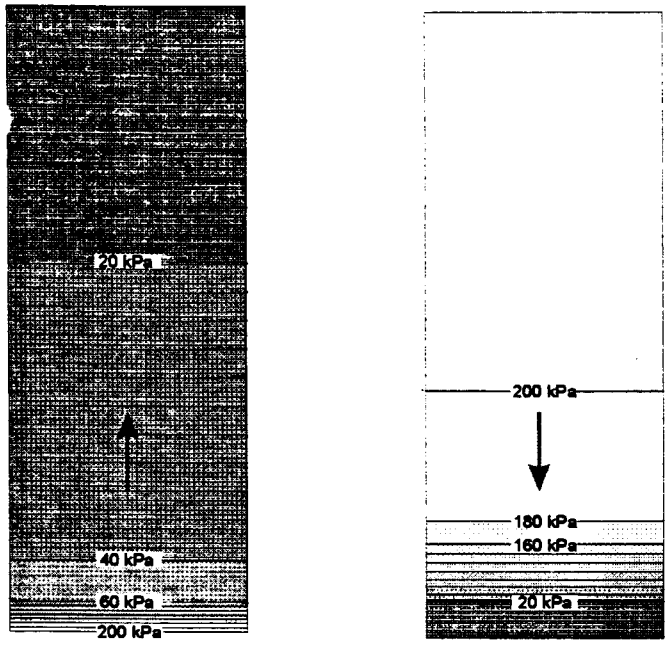

FIG. 16—*Distribution of soil suction throughout the ceramic sensor.*

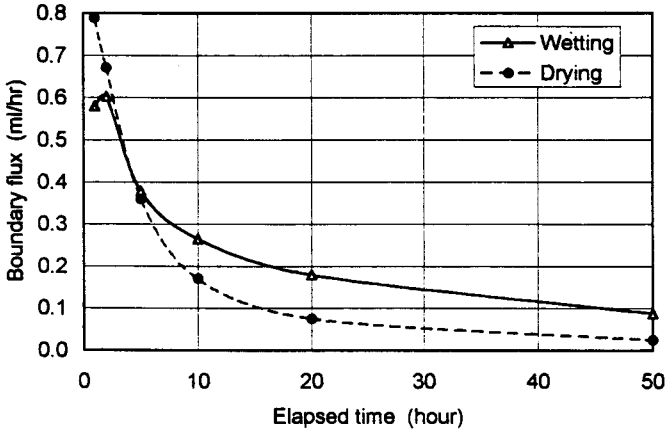

FIG. 17—*Computed boundary flux versus elapsed time for the soil suction sensor study.*

a result, the equalization time required for the initially dry sensor is less than the equalization time for the initially wet sensor.

The computed boundary flux versus elapsed time curves are shown in Fig. 17. At the beginning of the equalization process, the boundary flux for an initially wet sensor is much higher than the boundary flux of the initially dry sensor. However, the boundary flux of the wet sensor drops quickly with time and becomes less than the boundary flux of the dry sensor in less than 5 h due to the formation of the unsaturated zone near the boundary. This shows that the unsaturated zone causes the equalization time for an initially wet sensor to be longer than that for an initially dry sensor.

The influence of the unsaturated zone on the equalization time is dependent upon the change in water storage related to a change in soil suction. The higher of the water storage change, the stronger the influence of the unsaturated zone and the larger the different in equalization time between a dry and a saturated sensor. In Fig. 8*a*, it can be seen that for a silt soil the change in volumetric water content associated with a change in soil suction from 0 to 1000 kPa is about 0.35. This is higher than the volumetric water content change for a sand (i.e., which is 0.3) or a clay (i.e., which is less than 0.1). Therefore, the difference in the equalization time between a dry sensor and a saturated sensor for a silt is higher than that for a sand or a clay.

The amount of water transferred between the ceramic and the soil in order to equalize the suction values may also contribute to the longer equalization time for an initially wet sensor. For example, when the initial suction of the a soil is 200 kPa, the amount of water transferred for an initially saturated sensor is about 13.57 mL, whereas only 1.4 mL is needed for an initially dry sensor.

Conclusions

A finite element discretization was successfully used to predict the soil suction equalization process of soil suction during a sensor calibration. The results indicate that the equalization time required for calibration is primarily controlled by the hydraulic properties of the ceramic. The equilibrium time increases with an increasing applied suction due to a decrease in the coefficient of permeability of the ceramic.

Both laboratory suction measurements and numerical simulations indicate that in most cases the equalization time required for an initially dry sensor is less than the equalization time for an initially wet sensor. This is particularly true at high soil suctions. Numerical simulation also showed that the difference in equalization time is mainly caused by the unsaturated zone that develops at the boundary of the initially wet sensor at beginning of the drying process. The low coefficient of permeability in the unsaturated zone prevents water inside the wet sensor from flowing out, resulting a longer equalization time. The amount of water transferred between the ceramic and the soil may also result in a longer equalization time for an initially wet sensor.

References

Fredlund, D. G, Gan J. K.-M. and Li, W.-X., 1994, "Thermal Conductivity Suction Sensors—Design Consideration," *Proceeding of the 13th International Conference on Soil Mechanical and Foundation Engineering*, New Delhi, India, pp. 291–296.

Fredlund, D. G., Shuai, F., Yazdani, J., and Feng, M., 1998, "Recent Developments on a Sensor for the In Situ Measurement of Matric Suction," *51st Canadian Geotechnical Conference*, Vol. 1, pp. 81–86.

Fredlund, D. G. and Wong, D. K. H., 1989, "Calibration of Thermal Conductivity Sensors for Measuring Soil Suction," *ASTM Geotechnical Testing Journal*, Vol. 12, No. 3, pp. 188–194.

Fredlund, D. G. and Xing, A., 1994, "Equation for the Soil-Water Characteristic Curve," *Canadian Geotechnical Journal*, Vol. 31, pp. 521–532.

Fredlund, D. G., Xing, A., and Huang, S. Y., 1994, "Predicting the Permeability Function for Unsaturated Soils Using the Soil-Water Characteristic," *Canadian Geotechnical Journal*, Vol. 31, pp. 533–546.

Fredlund, M. D., 1999, *SoilVision User's Guide—A Knowledge-Based Database System for Soil Properties*, Version 1.0, SoilVision Systems Ltd., Saskatoon, Sask. Canada.

Geo-Slope, 1999, Seep/w Users Manual, Geo-Slope International Ltd., Calgary, Alberta, Canada.

Green, R. E. and Corey J. C., 1971, "Calculation Hydraulic Conductivity: A Further Evaluation of Some Predictive Methods," *Proceedings Soil Science Society of America*, Vol. 35, pp. 3–8.

Sattler, P. J. and Fredlund, D. G., 1989, "Use of Thermal Conductivity Sensor to Measure Matric Suction in the Laboratory," *Canadian Geotechnical Journal*, Vol. 26, pp. 491–498.

Wong, L. C., 1985, "Impact of Freeze-Thaw Cycles on the Permeability of Compacted Liner Materials," M.Sc. thesis, Department of Civil Engineering, University of Saskatchewan.

Xing, A. and Fredlund, D. G., 1994, "Numerical Modeling of a Thermal Conductivity Matric Suction Sensor," *ASTM Geotechnical Testing Journal*, Vol. 17, No. 4, pp. 415–424.